

# A 910MHz Injection Locked BFSK Transceiver for Wireless Body Sensor Network Using Colpitts Oscillator

M.Yousefi<sup>1</sup>

Z. D. Koozehkanani<sup>2</sup>

J. Sobhi<sup>3</sup>

<sup>1</sup> Ph.D. Research Engineering Student, Faculty of Electrical and Computer Engineering,  
University of Tabriz, Tabriz, Iran  
[m.yousefi@tabrizu.ac.ir](mailto:m.yousefi@tabrizu.ac.ir)

<sup>2</sup> Professor, Faculty of Electrical and Computer Engineering,  
University of Tabriz, Tabriz, Iran  
[zdaie@tabrizu.ac.ir](mailto:zdaie@tabrizu.ac.ir)

<sup>3</sup> Associate Professor, Faculty of Electrical and Computer Engineering,  
University of Tabriz, Tabriz, Iran  
[sobhi@tabrizu.ac.ir](mailto:sobhi@tabrizu.ac.ir)

## Abstract:

A 910MHz high efficiency RF transceiver for Wireless Body Area Network in medical application is presented in this paper. High energy efficiency transmitter and receiver architectures are proposed. In wireless body sensor network, the transmitter must have higher efficiency compared with the receiver because a large amount of data is sent from sensor node to receiver of the base station and smaller amount of data is received. Using colpitts oscillator in the proposed transceiver with injection-lock technique, the efficiency of transmitter and receiver has been improved. The designed transceiver consumes 1 mW at -6 dBm output with 5 Mbps data rate. Energy consumption of transmitter and receiver are 864 pJ/(bit×mW) and 114 pJ/bit, respectively. The proposed transmitter was designed in 0.18  $\mu\text{m}$  RFCMOS technology.

**Keywords:** High efficiency, Transceiver, Wireless body sensor network, Low power, High data rate

---

Submission date:13, Jan, 2015

Conditionally Acceptance date:8, Aug., 2015

Acceptance date:21, Dec., 2016

Corresponding Author: M.Yousefi

Corresponding author's address: Faculty of Electrical and Computer Engineering, University of Tabriz, Tabriz, Iran.



## 1. Introduction

Wireless body sensor network (WBSN) provides wireless connectivity among sensors used for the exhibition of vital signals of body and personal serves. Personal computer, cell phone, wireless local area network (WLAN), and internet network are personal serves used to connect with medical center and WBSN. Vital signal monitoring, diagnose assistant and the drug delivery are medical application of WBSN [1-4]. Fig.1 illustrates a typical scenario of WBSN application.

In typical WBAN applications, the distance between node and gateway is less than 3 meters and output power for transmitter is less than 1 mW. Sensor node is composed of sensing section, analog to digital converter (ADC), digital processor, and transceiver. Sensor node must be small to limit the required source energy. Since the transceiver is a block with higher power consumption, the design of an RF transceiver is challenging for the WBSN sensor node.

Low power digital communication systems typically use simple binary modulation schemes such as ON-OFF keying (OOK), binary frequency shift keying (BFSK), or binary phase shift keying (BPSK). The choice of modulation scheme determines the architecture of the transceiver. The OOK offers the low power solution because demodulation does not require an accurate reference signal. Although an OOK modulation system can consume extremely low power in receiver section, it is seldom used due to low data rates associated with long settling times and increased sensitivity to interferers [5-9]. FSK modulation is preferred for transceiver because of its better noise immunity. The injection-locked technique is used in receiver section which results in reduced dc power.

In most reported papers, figure of merit for transmitter is that how much energy is consumed for sending one bit assuming that error did not occur in data transmission. Conventional FOM does not take the transmit power into account. Transmitters that have a higher output power normally consume more dc power, which is a disadvantage. Through this work, an alternative FOM is used, denoted  $FOM_{TX}$ , which normalizes the energy efficiency (FOM) to the output power,  $P_{o[10]}$ . That is,

$$FOM_{TX} = DC \text{ power (mW)} / (\text{data rate} \times P_{out} \text{ (mW)}) \quad (1)$$

$FOM_{TX}$  has been used as a better factor to compare the low power transmitters [7-8].  $FOM_{TX}$  has units of  $J/(\text{bit} \times W)$ . High data rate wireless connectivity is required for applications like capsule endoscopy or multichannel biosensor recording. In order to maximize the life time, data rate and dc power must be respectively high and low.

Transmitter and receiver architectures with high energy efficiency are proposed to achieve high data rate with low power consumption. This paper is organized as follows: Section 2 describes the basic operation of the receiver and its blocks. Section 3 describes blocks of transmitter. Simulation results are presented in section 4. Finally, section 5 concludes the paper.

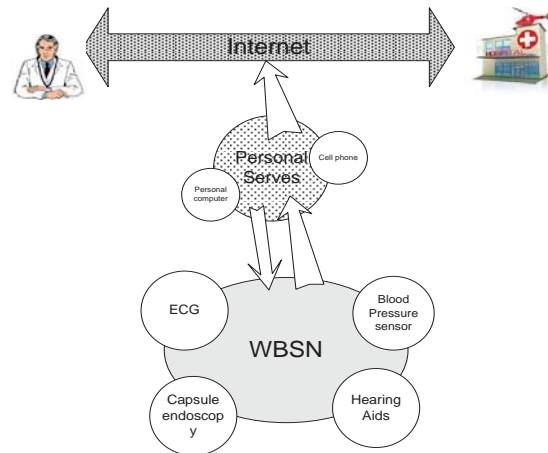


Fig.1. Typical WBSN

## 2. Receiver structure

In the designed receiver, BFSK modulation scheme is utilized, in which binary "1" is represented by frequency  $f_1$  and binary "0" is represented by frequency  $f_2$ . The transceiver adopts simple circuitry structure to save power. The receiver is composed of several major building blocks: the LO generation, ADC, envelop detector and the LNA and transmitter section composed of oscillator and power amplifier. The block diagram receiver is represented by Fig. 2.

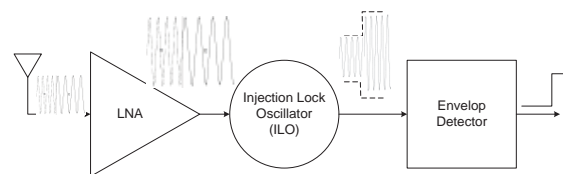


Fig.2. Block Diagram of Receiver

### 2.1. Injection-lock Receiver

The performance of the oscillator at  $\omega_0$  frequency is presented in paper [11]. When a periodic waveform at a frequency near  $\omega_0$  is injected to the oscillator, if frequency of injection signal differs from frequency of oscillator, the tank of oscillator needs to contribute phase shift. The circuit of Fig.3 exhibits a phase shift.

$$\theta = \frac{\pi}{2} - \tan^{-1}\left(\frac{L\omega}{R_p} - \frac{\omega_0^2}{\omega_0^2 - \omega^2}\right) \quad (2)$$

Since  $\omega_0^2 - \omega^2 \approx 2\omega_0(\omega_0 - \omega)$ ,  $L\omega/R_p = 1/Q$ , with  $\pi/2 - \tan^{-1}x = \tan^{-1}(1/x)$ , we have:

$$\tan \theta \approx \frac{2Q}{\omega_0^2} (\omega_0 - \omega) \quad (3)$$

If the input contains phase modulation, the phase shift can be obtained by replacing  $\omega$  in Equation 3 with the instantaneous input frequency,  $\omega + d\phi/dt$ :

$$\tan \theta \approx \frac{2Q}{\omega_0^2} \left(\omega_0 - \omega - \frac{d\phi}{dt}\right) \quad (4)$$

Consider the feedback oscillatory system shown in Fig 3(a), where the injection is modeled as an additive input. The output is represented by a phase-modulated signal having a carrier frequency of  $\omega_{inj}$ . The output is equal to:

$$\begin{aligned} V_x &= V_{inj,p} \cos(\omega_{inj}t) + V_{osc,p} \cos(\omega_{inj}t + \theta) \\ &= (V_{inj,p} + V_{osc,p} \cos \theta) \cos(\omega_{inj}t) - V_{osc,p} \sin \theta \sin(\omega_{inj}t) \end{aligned} \quad (5)$$

In the above equation,  $V_{inj}$  is amplitude of injection signal and  $V_{osc,p}$  is amplitude of output and  $\theta$  is the phase difference between the input and output.

Factoring  $(V_{inj} + V_{osc,p} \cos \theta)$  from Equation 5 and defining:

$$\tan \varphi = \frac{V_{osc,p} \sin \theta}{(V_{inj,p} + V_{osc,p} \cos \theta)} \quad (6)$$

rewriting Equation 5 as follows:

$$V_x = \frac{V_{inj,p} + V_{osc,p} \cos \theta}{\cos \varphi} \cos(\omega_{inj}t + \varphi) \quad (7)$$

With consideration that amplitude of the injection signal is smaller than the amplitude of output signal and also, the following relationships,

$$\cos \varphi = \sqrt{1 + \tan^2 \varphi} \quad (8)$$

$$\cos \varphi \approx (V_{inj,p} + V_{osc,p} \cos \theta) / \sqrt{V_{osc,p}^2 + 2V_{osc,p} V_{inj,p} \cos \theta} \quad (9)$$

output voltage is developed as:

$$V_x = \sqrt{V_{osc,p}^2 + 2V_{osc,p} V_{inj,p} \cos \theta} \cos(\omega_{inj}t + \varphi) \quad (10)$$

Upon traveling through the LC tank, this signal experiences a phase shift given by (7):

$$V_{out} \approx V_{osc,p} \cos \left\{ \omega_{inj}t + \varphi + \tan^{-1} \left[ \frac{2Q}{\omega_0} (\omega_0 - \omega_{inj} - \frac{d\phi}{dt}) \right] \right\} \quad (11)$$

Equating Equation 10 with  $V_{osc,p} \cdot \cos(\omega_{inj}t + \theta)$ , we obtained:

$$\theta = \varphi + \tan^{-1} \left[ \frac{2Q}{\omega_0} (\omega_0 - \omega_{inj} - \frac{d\phi}{dt}) \right] \quad (12)$$

From Equation 6 we get:

By having,

$$\frac{d\varphi}{dt} = \frac{V_{osc,p}^2 + V_{osc,p} V_{inj,p} \cos \theta}{V_{osc,p}^2 + V_{osc,p} V_{inj,p} \cos \theta + V_{inj,p}^2} \frac{d\theta}{dt} \approx \frac{d\theta}{dt} \quad (13)$$

$$\tan(\theta - \varphi) = \frac{V_{inj,p} \sin \theta}{(V_{inj,p} + V_{osc,p} \cos \theta)} \approx \frac{V_{inj,p} \sin \theta}{V_{osc,p}} \quad (14)$$

Therefore, from Eqs. (11)–(13), we achieve:

$$\frac{d\theta}{dt} = \omega_0 - \omega_{inj} - \frac{\omega_0}{2Q} \frac{V_{inj,p}}{V_{osc,p}} \sin \theta \quad (15)$$

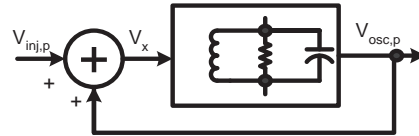
For the oscillator to lock to the input, the phase difference should not change so  $d\theta/dt$  is zero.

$$\omega_0 - \omega_{inj} - \frac{\omega_0}{2Q} \frac{V_{inj,p}}{V_{osc,p}} \sin \theta = 0 \quad (16)$$

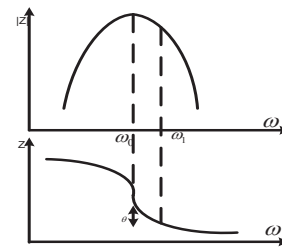
In the lock range,

$$\omega_L = |\omega_0 - \omega_{inj}| \leq \frac{\omega_0}{2Q} \frac{V_{inj,p}}{V_{osc,p}} \quad (17)$$

where  $\omega_L$  is locking bandwidth and  $\omega_0$  is operating frequency, and  $Q$  is the quality factor of oscillator [12]. For example, in this application, the receiver's oscillator has a free-running differential peak-to-peak swing of 1.2V with quality factor of 10 and resonance at 910 MHz, the injected signal into the oscillator will have 50 mVp-p swing. The lock range  $\omega_L$  is 2.25 MHz.



(a)



(b)

**Fig.3. Output amplitude of Injection Lock Oscillator (ILO) with respect to incident frequency in the lock range[10].**

## 2.2. LNA and Amplifier

The LNA transistor level schematic is shown in Fig.3. Low noise figure, high gain, good linearity, good matching and low power LNA is a requirement for the receiver. The LNA uses common source structure with cascode transistor. The  $L_1$  and  $C_1$  are used for input impedance matching with impedance of antenna (50 ohm) and filtering input signal. The common source stage of LNA is realized for

amplifying, also, the cascode transistor  $M_2$  is used to isolate antenna from load. As shown in Fig.3, the capacitor  $C_3$  serves as a dc block. For tuning the overall gain of LNA block, an inverter with resistive feedback has been used. In the proposed transceiver, the designed LNA has  $280 \mu\text{W}$  dc power and  $-30 \text{ dB}$   $S_{11}$ . To maintain operating frequency range of receiver with minimum input power, the LNA gain should be high enough. The proposed LNA has  $40 \text{ dB}$  variable voltage gain which can be adjusted by 4 digital signals. Finally, the output voltage of LNA is injected to current source of the oscillator.

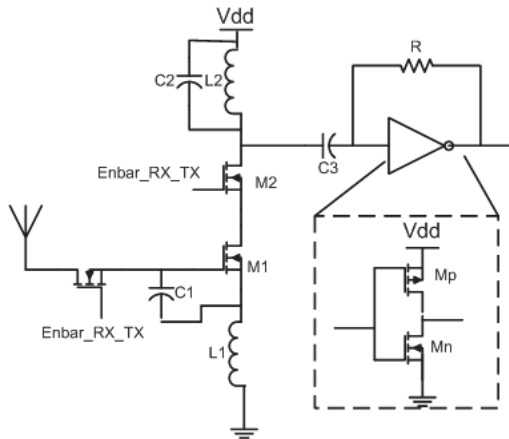


Fig.4. The circuitry of LNA

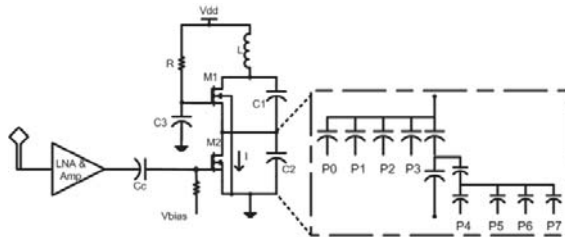


Fig.5. A schematic of Colpitts oscillator

### 2.3. Injection locked oscillator

Injection locked oscillator is the block playing a key role in the proposed receiver. A schematic of proposed injection locked Colpitts oscillator is illustrated in Fig.4. The Colpitts oscillator uses a pair of capacitors to produce the regenerative feedback necessary for oscillation. The amplifier output is developed across  $C_1$ , and feedback voltage is developed across  $C_2$ . The voltage across  $C_2$  is  $180$  degrees out of phase with the voltage across  $C_1$ , thus feedback is regenerative. The incident signal is injected on the gate terminal of transistor  $M_2$ .

### 2.4. Envelop detector and one bit-ADC

The envelop detector composed of one transistor with diode connection, resistor, and capacitance. The

resistor and capacitor act as a low pass filter. The circuitry of envelop detector is shown in Fig.5. The envelop detector noise has a negligible effect on noise figure of the receiver. The amplitude of envelop detector is detectable [13]. In the following envelop detector, the common source amplifier is used. The envelop detector and common source are used to convert amplitude-modulated signal to DC baseband signal. The output signal of envelop detector section converted to 1 bit data with an ADC.

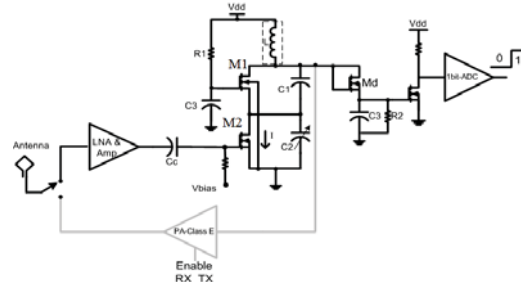


Fig.6. Block diagram of the receiver section

## 3. Transmitter section

Fig.6 illustrates the schematic of the transmitter. Major blocks of the transmitter are oscillator and power amplifier. The  $5 \text{ Mbps}$  modulated FSK signal with constant envelope is generated by the transmitter.

### 3.1. Oscillator

In the proposed transmitter, the Colpitts oscillator is used to generate carrier frequency. To decrease area, the Colpitts oscillator of the receiver is reused in the transmitter. In the Colpitts oscillator, the transistor  $M_2$  of gate terminal oscillates at frequency  $\omega_0$ . This frequency is equal to the frequency of output voltage. In the LC oscillator, this resonance frequency is as output voltage frequency. As a result, the injection signal frequency is not different from oscillator frequency. That is suitable for design of high efficiency transmitter. As shown in Fig.4, the digital controlled oscillator (DCO) can be tuned by 8-bit capacitor bank. The oscillator has  $-164 \text{ dBc/Hz}$  phase noise, while consuming  $404 \mu\text{A}$  from  $0.7 \text{ V}$  power supply.

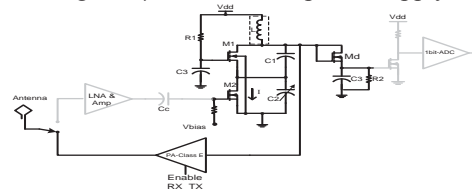


Fig.7. The circuitry of the proposed transmitter power amplifier.

### 3.2. Power amplifier

To transmit the modulated signal, in the proposed transceiver, power amplifier reported in [14-16] has been used. Reported topologies for WSN applications are invariably non-linear to achieve the best efficiency. Tuned circuits are employed in the output matching circuitry to block the non-linear products at the harmonic frequencies. Switched power amplifier like inverter with or without a current source as reported in [14-17], exhibits good efficiency since the conduction angle is very low. Also, termed as push-pull topology, it maximizes  $g_m/I_D$  as the effective  $g_m$  is doubled, as it is the sum of PMOS and NMOS reusing the current. Efficiency of power amplifier is output power versus dc power PA.

The proposed power amplifier has two transistors from  $V_{dd}$  to ground thus minimum  $V_{dd}$  required is  $(V_{GS}+V_{DSAT})$ , and hence is suitable for low supply voltage applications. While the proposed structure for power amplifier has good efficiency for OOK modulation, it suffers from poor isolation from output to input. Variations in the load impedance due to component variations, affects the input impedance, input swing, gain, dynamic current consumption, and the frequency of the oscillator due to pulling. We have designed this structure as shown in Fig.7. In this PA, the matching block is implemented on-chip.

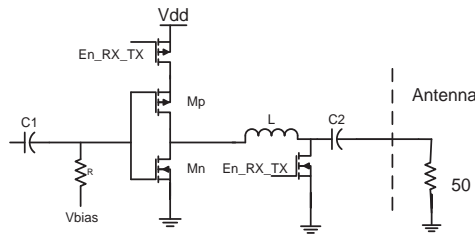


Fig. 8. The circuitry of power amplifier

Table. 1. Summary of the proposed transceiver's characteristics

Parameters	Value
Power supply	0.7 V
Technology	0.18 $\mu\text{m}$
Modulation	BFSK
Maximum Data Rate	5 Mb/s
Carrier Frequency	910 MHz
Power consumption TX (mW)	1.037
Power consumption RX (mW)	0.570
Output Power (mW)	0.24

### 4. Results

The proposed transceiver has been designed on a 0.18  $\mu\text{m}$  RFCMOS process. The oscillator has a 910 MHz output signal with minimum 0.4 V swing. In Table1, a summary of proposed transceiver's characteristics is represented. Fig. 9 shows that the oscillator has -164 dBc/Hz phase noise while consuming 404  $\mu\text{A}$  from 0.7 V power supply. In Fig. 10, waveform of received signal pattern and output envelop detector are shown with "1010" data message and 5 Mbps data rate. The 912 MHz and 912.6 MHz are used for sending "0" and "1". The difference in enveloping voltage of envelop detector in "0" and "1" is 5 mV. The oscillator consumes 0.26 mA from the 0.7 V power supply.

The output power of transmitter is -6.2 dBm with 50 ohm load with TX efficiency of 23%. Fig. 11 shows the efficiency of TX and PA with output level. For changing output power  $V_{ctrl}$  and  $I_{bias}$ , current source oscillator is used. As shown in Fig.11, the efficiency of TX is decreased with the decrease output level. For changing output level,  $I_{bias}$  ( $I_{bias}$  is current of oscillator) is better than  $V_{ctrl}$  ( $V_{ctrl}$  is power supply of power amplifier).

Fig.12 plots the DCO frequency with digital control signals. The DCO frequency can be tuned to a desired frequency over the range of 908 to 919 MHz. In fine calibration, frequency steps are nonlinear. The accuracy of DCO is maximum 100 kHz per one bit and also, for some steps, step of altering frequency is under 100 KHz. With 5 Mbps data rate and 8 bit control signal the required time for calibration is 50  $\mu\text{s}$ . This calibration time is suitable in WBSN [15-16].

The performance comparison with other low power transmitters is shown in Table 2. Proposed transmitter FOM is 864 pJ/(bit $\times$ mw). All elements of the proposed transceiver are on chip elements except the inductor of the oscillator. If all inductors are designed off chip (High Q), the FOM of the transceiver will be better than the proposed transceiver. But the proposed transceiver consumes smaller area with favorable performance. Fig.14 shows spectrum output transmitter for 910 MHz fundamental harmonic and -6 dBm output power.

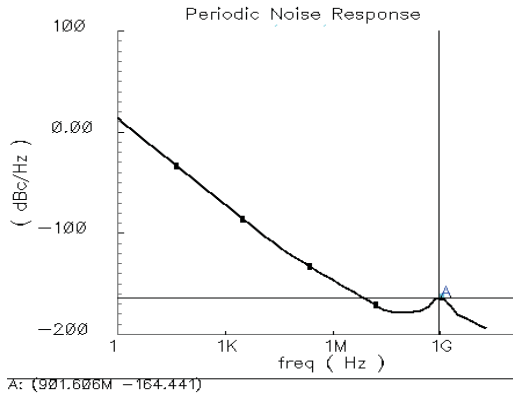


Fig. 9. Phase Noise of oscillator

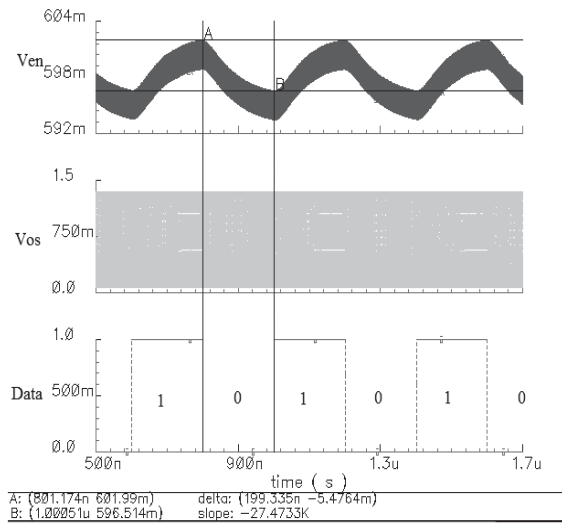


Fig. 10. Waveform of data message with "1010" pattern and 5 Mbps data rate frequency

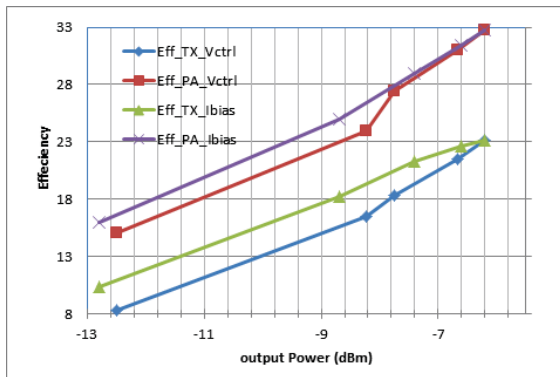


Fig. 11. Efficiency of the transmitter and PA with respect to output power

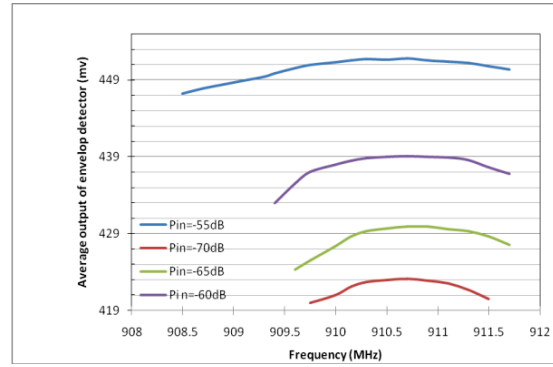


Fig. 12. Average of output of envelop detector with respect to injection frequency

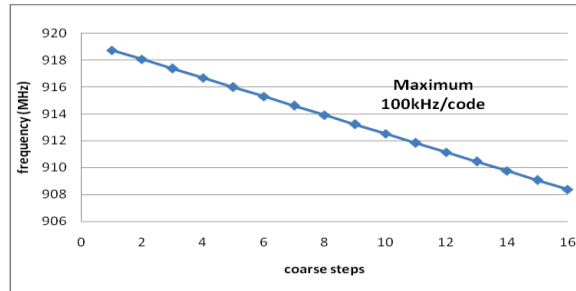


Fig. 13. Frequency tuning curve of DCO with respect to coarse steps

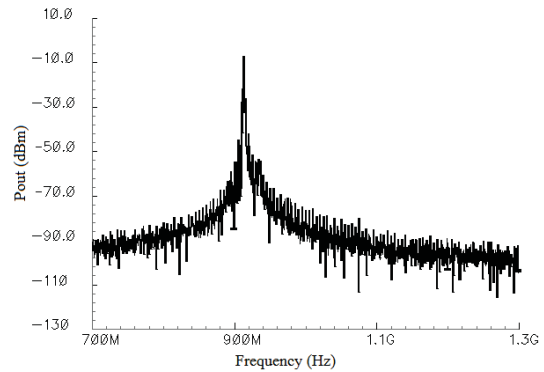


Fig. 14. Spectrum Output transmitter

## 5. Conclusion

A highly efficient BFSK transmitter has been proposed for wireless body sensor network.  $FOM_{TX}$  is  $864 \text{ pJ}/(\text{bit} \times \text{mW})$ . The proposed receiver employs injection lock technique which decreases DC power of the receiver. In the proposed transceiver, Colpitts oscillator has been used to generate RF carrier. In the Colpitts oscillator the output of the oscillator and injection node have the same frequency that improves the efficiency of TX. All elements of the proposed transceiver are on chip elements except the inductor of the oscillator.

**Table 2. Performance comparison of transceivers.**

Ref.	12	19	10	This work
$F_{RF}$ (GHz)	2.4	0.4	0.9	0.91
Tech. ( $\mu\text{m}$ )	0.13	0.18	0.18	0.18
DR(Mbps)	0.3	0.25	5	5
Mod.	FSK	FSK	BFSK	BFSK
Sen. (dBm)	--	-70	-73	-70
P. Supply (V)	0.4	0.7	0.7	0.7
Pdc_RX (mW)	1	0.49	0.42	0.57
Pdc_TX (mW)	0.33	0.4	0.7	1.037
Out. Pow. (mW)	0.3	0.025	0.1	0.24
$FOM_{TX}$ (nJ/(bit*mW))	11.1	64	1.4	0.86
$FOM_{RX}$ (pJ/bit)	---	1960	84	114

## References

- [1] W. Wong, D. McDonagh, G. Kathiresan, O. Omeni, O. El-Jamaly, T. K. Chan, P. Paddan, and A. Burdett, "A 1 V, micropower system-on chip for vital-sign monitoring in wireless body sensor networks", in Proc. IEEE Int. Solid-State Circuits Conf. San Francisco, pp. 138-139, 2008.
- [2] Y. Yang, Y. Huang, H. Liao, T. Wang, P. Huang, C. Lin, Y. Wang, S. Lu. "A release-on-demand wireless CMOS drug delivery SoC based on electrothermal activation". IEEE International Solid-State Circuits Conference. 2009. pp: 288-289.
- [3] Vouilloz, M. Declercq and C. Dehollain "A low-power CMOS super-regenerative receiver at 1 GHz", IEEE Journal of Solid-State Circuits, vol. 36, no. 3, pp.440-451, 2001.
- [4] Otis et al., "A 400 $\mu$ W-RX, 1.6mW-TX Super-Regenerative Transceiver for Wireless Sensor Networks" International Solid State Circuits Conference, Digest of Technical Papers, pp. 396-397, Feb 2005.
- [5] J.-Y. Chen , M. P. Flynn and J. P. Hayes "A fully integrated auto-calibrated super-regenerative receiver in 0.13  $\mu\text{m}$  CMOS", IEEE J. Solid-States Circuits, vol. 42, no. 9, pp.1976-1985 2007
- [6] J. Bohorquez, A.P. Chandrakasan, and J.L. Daeson, "A 350 $\mu$ W CMOS MSK transmitter and 400 $\mu$ W OOK super-regenerative receiver for medical implant Dig. Tech Papers, 2009, pp. 36-37.
- [7] M. Vidojkovic, X. Huang, P. Harpe, S. Rampu, C. Zhou, L. Huang, K. Imamura, B. Busze, F. Bouwens, M. Konijnenburg, J. Santana, A. Breeschoten, J. Huisken, G. Dolmans and H. de Groot, "A 2.4GHz ULP OOK Single-chip Transceiver for Health care Applications" IEEE ISSCC Dig. Tech. Papers, 2011, pp. 458-459.
- [8] J. Bae , L. Yan and H.-J. Yoo "A low energy injection-locked FSK transceiverwith frequency-to-amplitude conversion for body sensor applications", IEEE J. Solid-State Circuits, vol. 46, no. 4, pp.928 -937, 2011.
- [9] Rahimpour H, Gholami M, Miar-Naimi H, Ardeshir G. Design of a Novel DLL-Based Frequency Multiplier for High Speed Applications. Journal of Iranian Association of Electrical and Electronics Engineers. 2015; 12 (2) :39-46
- [10] M.K. Raja, et al., "A 52 pj/bit OOK transmitter with adaptable data rate," ASSCC 2008, pp.341-344, Nov
- [11] B. Razavi, A study of injection locking and pulling in oscillators, IEEE J. Solid-State Circuits, vol. 39, No. 9, pp. 1415-1424, Sep. 2004.
- [12] B. Cook, A. Berny, A. Molnar, S. Lanzisera and K. S. J. Pister "Low-power 2.4 GHz transceiver with passive Rx front-end and 400 mV supply", IEEE J. Solid-State Circuits, vol. 41, no. 12, pp.2757-2766, 2006.
- [13] Daly, Denis Clarke. "An energy efficient rf transceiver for wireless microsensor networks". Diss. Massachusetts Institute of Technology, 2005.
- [14] B.P. Otis, Y.H. Chee, R. Lu, N.M. Pletcher, and J.M. Rabaey, 'An Ultra-Low Power MEMS-Based Two-Channel Transceiver for Wireless Sensor Networks', Proceedings of the Symposium on VLSI Circuits, Honolulu, Hawaii, 2004.
- [15] J. P. Carmo , N. S. Dias , H. R. Silva , P. M. Mendes , C. Couto and J. H. Correia "A 2.4-GHz low-power/low-voltage wireless plug-and-play module for EEG applications", IEEE J. Sensors, vol. 7, no. 11, pp.1524-1531, 2007.
- [16] Moazedi M, Abrishamifar S A. Wide Band Delay-Locked-Loop with Self-Biased Mismatch-Free Charge-Pump. Journal of Iranian Association of Electrical and Electronics Engineers. 2012; 9 (1) :1-12
- [17] C Angeloni, P O Riley and E D Krebs. "Frequency Content of Whole Body Gait Kinematic Data." IEEE Trans. Rehabilitation Engineering, 2 (1), pp. 40-46, 1994.
- [18] J. Ryu , M. Kim , J. Lee , B. Kim , M. Lee and S. Nam "Low-power OOK transmitter for wireless capsule endoscope", Proc. IEEE MTT-S Int. Microw. Symp . Exhib., pp.855-858, 2007.
- [19] J. Bae, N. Cho, and H.-J. Yoo, "A 490  $\mu$ W fully MICS compatible FSK transceiver for implantable devices," in Symp. VLSI Circuits